New J. Chem., 1994, 18, 1125-1134

Organic-inorganic nanocomposites for micro optical applications

H. KRUG and H. SCHMIDT

Institut für Neue Materialien, Im Stadtwald, Gebäude 43, 66123 Saarbrücken, Germany.

Received November 8, 1993.

Abstract. – Control of phase separation during the sol-gel process is an essential issue in case of organic-inorganic hybrid materials for optical and microoptical applications. In order to minimize optical losses by scattering effects, phase dimensions are controlled to be in the nm range. The use of nanoparticles allows to adjust the index of refraction only by changing particle contents and buffer and gladding coatings can be built up in combination with waveguiding films. Examples are given for the control of the conversion behavior of C=C double bonds of methacrylate functionalized alkoxides in case of photopolymerization, which is an other essential issue to taylor material properties. Patterning techniques are presented to get micro optical devices like strip-waveguides, diffraction gratings and Fresnel micro lenses.

Key words : Polymerization behavior, embossing, laser writing, holography.

Résumé. – Nano-particules organiques-inorganiques utilisées en micro-optique. Dans le cas d'applications en optique ou micro-optique, le contrôle de la séparation de phase dans le procédé sol-gel est un point essentiel. Afin de minimiser les pertes optiques par diffusion, la dimension des phases doit être maintenue dans la gamme du nanomètre. L'utilisation de nano-particules permet d'ajuster l'indice de réfraction en changeant la quantité de particules. Des revêtements tampon peuvent être élaborés en combinaison avec des films guide d'onde. Des exemples sont donnés pour le contrôle de la conversion par photopolymérisation des doubles liaisons C=C d'alkoxydes fonctionnalisés par un groupement méthylméthacrylate, ce qui est un autre point essentiel pour ajuster les propriétés des matériaux. Des techniques de gravure sont présentées pour élaborer des dispositifs optiques tels que des guides d'onde, des réseaux de diffraction et des micro-lentilles de Fresnel.

Introduction

The industrial fabrication of passive and active optical devices like Y-couplers, gratings, lenses, interferometers, amplifiers and frequency doublers is strongly influenced by the development and integration of new materials and technologies. This is limited by high development costs and small market volumes as these materials are normally not produced in tonnage but in small quantities. Furthermore integration of different optical functions requires the combination of different materials which has as a consequence very complex and cost intensive processing techniques. Sol-gel processing of organic-inorganic composite materials gives an attractive possibility to synthesize materials for micro-optical applications, as the combination of organic and polymer chemistry with sol-gel chemistry opens an almost endless possibility of variations in organic groupings and reaction conditions. Structural variations, which are directly correlated to material properties can be introduces by the choose of bonds between the organic and inorganic phase, the phase dimensions and type of matrix. regarding to these possibilities, it is essential that sol-gel chemistry leads to large changes in material properties by just changing chemical reaction parameters which is a useful tool to simply scan a wide range of material properties.

Non-reactive organic groupings act as network modifiers which for example in case of spin-on glasses lower the densification temperature to 200-300°C and allow thick film preparation of more than 20 μm by avoiding inner mechanical stresses. Organic modification with polymerizable chelating ligands can be for example introduced by alkoxy dicarbonates or methacrylates which act as complexing agents and form coordinative bonds. Inorganic ions can be incorporated by amine

complexes as chelating ligands. Stable bonds to colloids allow the introduction of colloidal particles into sol-gel precursor and is another interesting principle for the synthesis of a variety of multiphase nanocomposites; Besides a direct cross-linking of the reactive organic groupings it is also possible to build up organic chains by the addition of organic monomers and oligomers which do not only influence the morphology of the material but also in dependence of their kind influence thermal, mechanical and optical properties.

The recently increasing attention to inorganic-organic hybrid materials for optical applications is manifested in a lot of publications, which show the broad application spectrum of this material group in the optical field. Stabilization effects of a such a hybrid matrix for organic dye molecules was shown by Sanchez [1]. Levi et al. could show a remarkable stabilization effect of photochromic dyes [2], the same result was found by Hou [3] and Altman et al. in matrices based on methacryloxy silane systems with Rhodamine 6G [4]. Stabilization effects with a variety of dyes in MMA impregnated silica matrices after polymerization of the MMA species could be found by Reisfeld and coworkers [5]. Similar composites were prepared by Mackenzie and Klein [6,7] χ^3 polymers were reinforced in a sol-gel inorganic backbone matrices by Prasad [8]. To reduce shrinkage rates of pure inorganic sol-gel materials, TiO_2/SiO_2-polyethylene glycol composites were used fir embossing CD–ROMs [9]. An other composite material with an index of refraction $n_D = 1.73$ was produced by Wilkes et al. by combination of diamino diphenyl sulfone with TiO_2 sol-gel materials [10]. Spanhel et al. could prepare photoluminescent CdS semiconductor quantum dots in Ormocers using bifunctional ligands as surface modifiers [11], similar results were obtained by Mackenzie [6].

All these examples realize two different approaches to get an organic-inorganic composite material. The first one is that of an interpenetrating network of oligomeric units of both organic and inorganic parts. The second one is an nanoparticles or colloids containing sol-gel matrix. These particles can be prepared in vitro and can be mixed with the matrix material or can be generated in situ in the matrix during the sol-gel process. It is not obvious to get narrow size distribution of such generated particles but Sanchez [13], Rinn [14] and Strehlow [15] showed results indicating a model for narrow size distribution based on surface energy control by coordinative ligands. This surface modification by coordinative ligands is a powerful tool to control precipitation and particle size growing and is the key to open optical applications to organic-inorganic hybrid materials. In this context, Sanchez could show that β-dicarbonyl ligands in combination with Zr-alkoxides allow to tailor Zr nanoparticles between several and 50 nm which can be incorporated into inorganic-organic sol-gel matrices. The same results was found by Schmidt et al. for methacrylic acid complexed Zr alkoxides [16]. The fundamental understanding of particle formation, phase separation behavior and particle growing mechanisms is necessary for property tailoring, if these materials should be competitive to up to date optical materials.

General requirements on optical material properties

Materials for optical applications in information and communication technologies should provide several properties to be able to be competitive on the market. As already mentioned, they should be producible in small quantities without high costs. In contrast to f.e. complex processing techniques like physical or chemical vapor deposition, simple coating techniques like spin-on or dip-coating would be preferable. Beside low optical losses the possibility of index matching by simple means to produce buffer, waveguiding and gladding material is necessary to be independant of the substrate material and to eliminate or diminish the influence of surface roughness of the substrate and to protect the waveguiding material from environmental influences. In order to get materials for non linear optical applications, it should be usable as a matrix for chromophores, quantum dots, lanthanides and lasing dyes.

For all these applications, the fabrication of optical low loss materials is essential. Therefore the different parameters contributing to this optical loss will be mentioned in detail. In principle, it can be distinguished between volume induced and surface induced scattering losses. Volume induced losses are given by randomly isotropic fluctuations of the index of refraction or a second phase of different index of refraction with a characteristic correlation length of these volume inhomogeneities. Surface induced scattering losses are given by random deviations in the waveguide walls. All these different scattering losses superimpose and give in a sum the total attenuation. Calculations presented by Roncone et al. [17] give guidelines for how well surface roughness and refractive index inhomogeneities must be controlled to fabricate low loss mono mode waveguides with losses < 1 dB/cm. Surface roughness must be less then 1 nm with typical correlation length less then 100 nm, for index inhomogeneities typical values are $\delta n < 0.01$ with correlation length < 10 nm. In case of a second high refractive phase, phase dimension and difference of index of refraction to the matrix material are the dominating factors as the resulting attenuation by Rayleigh scattering for non-absorbing material is given

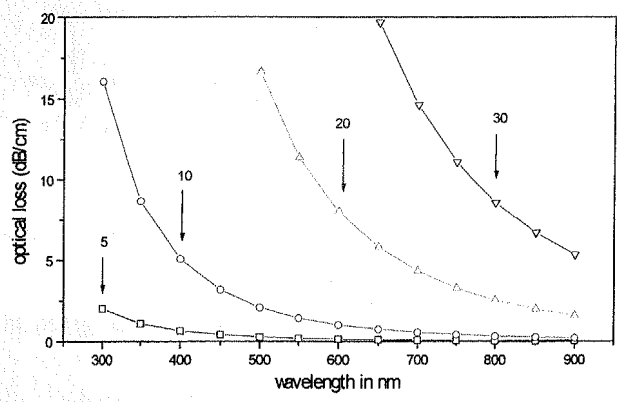

Figure 1. – Optical loss in dependance of wavelength for particle diameters of 5, 10, 20 and 30 nm (refractive index of the particles) 10% volume fraction in a matrix with index of refraction of 1.5.

by equation 1.

$$\frac{I}{I_0} = \exp -4\frac{\pi^4}{\lambda^4}\left[\frac{n_p^2 - n_m^2}{n_p^2 + 2n_m^2}\right] d^3 C_v l \qquad (1)$$

with λ: used wavelength n_p: refractive index of particles, n_m: refractive index of the matrix, d: particle diameter, c_v: volume fraction of the particles in the matrix, l: length of trace of light or sample thickness. As can be seen from equation 1, scattering losses are inverse proportional to 4th power of the used laser light which is the reason to use NIR wavelength of 1 300 nm and 1 500 nm in communication technology to reduce volume losses just by using higher wavelength. As can also be seen from equation 1 δn between the second phase and the matrix in an other dominating factor for volume losses in case of composite materials. The number value for the optical loss can easily be calculated by equation 2 (if l from equation 1 is set to 1 cm).

$$\frac{dB}{cm} = \frac{1}{10}\log\left(\frac{I}{I_0}\right) \qquad (2)$$

Calculated results of optical losses given by Rayleigh scattering using equation 1 and equation 2 for different particle diameters of the second phase (refractive index = 2.2, 10% volume fraction in a matrix with index of refraction = 1.5) is shown in Figure 1.

It is evident, that for a minimization of optical losses given by Rayleigh scattering, particle diameters must be less than 10 nm with narrow size distribution to eliminate losses by larger particles. These calculations are only valid for well dispersed systems, every agglomeration will strongly increase optical losses and has to be avoided.

To resume the most important requirements for composite materials in optics, one can say that surface roughness, which is a property not only of the material structure but can also be influenced by the used coating technique and which is in case of composite materials influenced by particle size has to be minimized. The control of chemical inhomogeneities, which are responsible for index fluctuations has to be optimized through chemistry and processing and for composite materials, minimum particle size has to be realized. In the following chapter, an example is given for the tailoring of an organic-inorganic nanocomposite material which fulfills most of these requirements.

Material synthesis and reaction control

In case of highly reactive alkoxides like $Zr(OR)_4$, simple addition of water leads to a precipitation of ZrO_2aq which is not acceptable to prepare homogeneous composite materials. Therefore, the reactivity of the Zr-component has to be slowed down which can be done by complexation with methacrylic acid. It is known [18], this chelating complex is stable against hydrolyzation. In the presence of latent water in a prehydrolyzed and condensated silane, the Zr alkoxide itself can be hydrolyzed and condensated without precipitation and well dispersed ZrO_2 particles of only some nm in diameter can be obtained [19]. If organically modified silanes are used, the methacrylic component at the surface of these particles can be used to copolymerize with the organic species of the organo silane.

In the following experiments, methacryloxypropyltrimethoxysilane (MPTS,I) was used as matrix material in combination with methacrylic acid (III) complexed zirconium propoxide (II). In a first step, 1 mol of MPTS is hydrolyzed and condensated with a slow addition of 0.5 N HCL. The water content is followed by Karl-

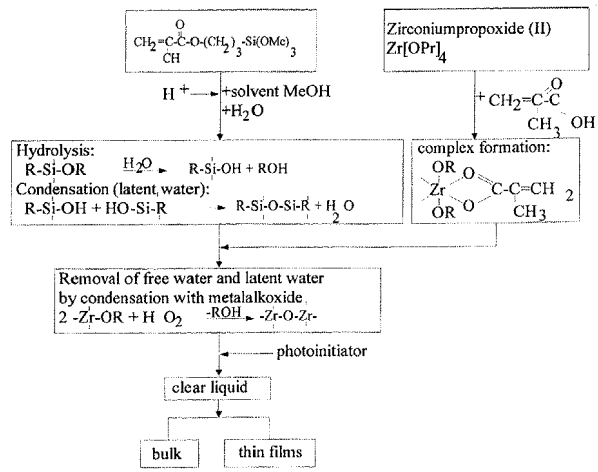

Figure 2. – Schematic float-chart of the controlled synthesis of an organic-inorganic nanocomposite with an alkoxysilane and a zirconium-alkoxides.

Fischer titration to determine the time after water content has minimized. In a second step, 1 mol zirconium propoxide is complexed with 1 mol methacrylic acid. In the used alkoxide precursor, the Zr-alkoxide content was 70 weight %. The complexed Zr alkoxide was mixed with the controlled condensated silane in different mol % under stiring and water was added. In order to initialize photopolymerization in further processing steps, a photoinitiator, which is optimized for the used light source is added. After stirring for several hours, ethanol or an other alcohol can be added as solvent to adjust the viscosity of the solution. All this work was done in a room which was specially prepared to handle photosensitive materials. Films can be prepared by simple techniques like spin-on or dip coating. Thin optical films with patterns for micro-optical applications can be produced by different patterning techniques which will be presented in detail in the following chapter. A schematic float chart of this soft chemical synthesis route is shown in Figure 2.

The hydrolysis of the organo alkoxy silane MPTS was followed by Karl-Fischer titration (H_2O content determination) to get the optimum time (minimum water content) for the addition of the complexed Zr-alkoxide (Fig. 3).

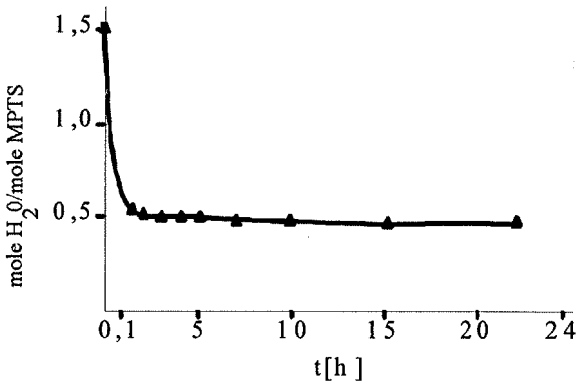

Figure 3. – H_2O concentration in the hydrolysis reaction of MPTS-silane as a function of time in the hydrolysis reaction (after 9, 10).

As can be seen from Figure 3, the minimum time before addition of the complexed Zr-alkoxide is at least about 1 h. If the component is added earlier, precipitation can not be avoided.

The condensation behavior of the silane before addition of the Zr/MAS component and of the MPTS/Zr/MAS composite was followed by ^{29}Si-NMR as the amount of two and three-dimensional crosslinking during condensation is an essential parameter for further interpretation of material properties. Network formation and terminology for species measured by NMR are given schematically in Figure 4. Measured chemical shifts and

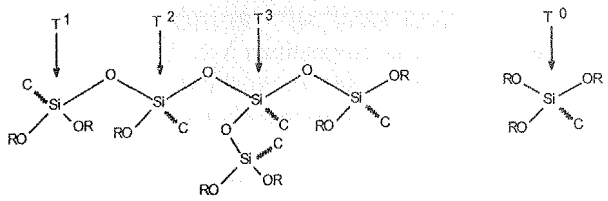

Figure 4. – Network formation by hydrolyzation condensation of the MPTS alkoxide with measurable NMR signals.

relative intensities for the different species are given in Table I.

Table I. – Measured NMR species with chemical shift and related intensities for the controlled condensated MPTS alkoxide and the MPTS/ZR/MAS composite.

Species	MPTS-sol	MPTS/Zr/MAS-sol
T0	42-44 (0%)	42-44 (0%)
T1	48.7-50.6 (38.2%)	48.8-50.7 (40.2%)
T2	54.8-59.3 (54.3%)	54.7-59.3 (54.5%)
T3	66.8-69.0 (7.6%)	66.3-68.5 (5.3%)

As can be seen from Table I, no T0 species, which corresponds to uncondensated monomers, can be found after hydrolyzation and condensation for both the pure MPTS as for the MPTS/ZR/MAS system. For both systems almost only T1 and T2 species with a small amount of T3 can be found. From the intensity of the signals can be followed, that the inorganic polymer system is purely three-dimensionally crosslinked and almost only two dimensional low molecular chains of dimers and polymers are formed by the condensation process. The presence of dimers and low molecular inorganic polymers can be concluded as the relation of the intensities of these two signals should be much higher for the T2 for long two-dimensional chains. As a consequence the material in the gel state should behave like a thermoplast which is essential for further processing of photopolymerization.

Particle diameter of the ZrO_2-particles, which are formed by the in situ condensation of the ZR/MAS in the MPTS matrix is measured in the sol state by photon correlation spectroscopy to be about 4 nm. No particles can be detected for both the pure MPTS matrix nor for the complexed ZR/MAS system before mixing.

After controlled hydrolyzation and condensation to build up the inorganic backbone of the material, formation of the organic network (organic part of the MPTS as well as of the ZR/MAS) can be induced by photopolymerization. By light illumination, the photoinitiator is transformed to radicals which activate the C=C double bonds of the methacrylate groupings. The degree of conversion (extend of polymerization) can be measured by the quantities

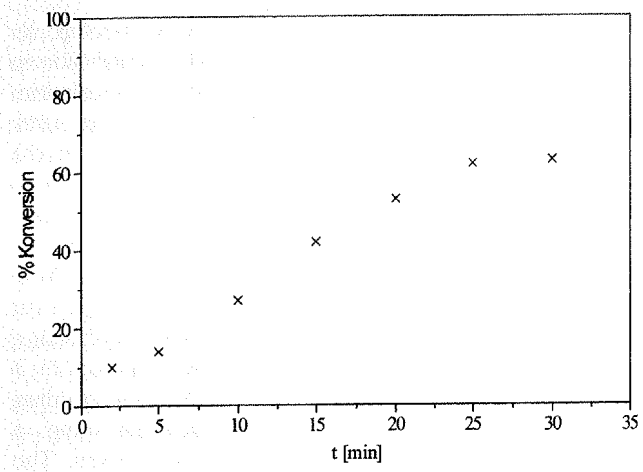

Figure 5. – Conversion rate of a system MPTS/ZR/MAS measured IR-spectroscopically at room temperature.

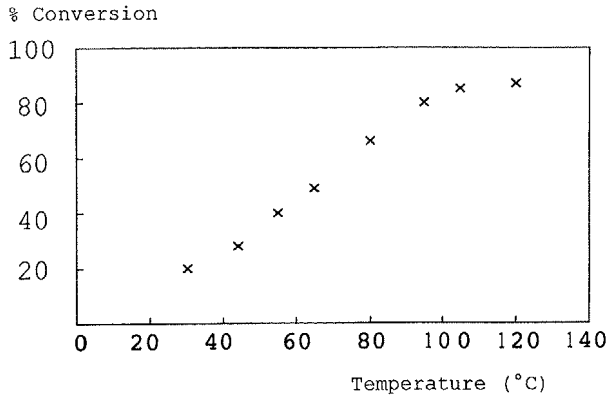

Figure 6. – Conversion in dependence of temperature during UV-polymerization.

of unreacted methacrylate groups using IR-spectroscopy. This technique is based on the decrease of C=C double bond absorption at 1 635-1 640 cm^{-1} by the radical chain polymerization. As a reference, the C=O absorption peak, which does not change during polymerization, was used. A typical curve obtained by this technique for the system MPTS/ZR/MAS is shown in Figure 5. The conversion behavior is comparable to photopolymerizable methacrylate based organic monomer systems, which are intensively investigated in dental restauration medicine.

Directly after the start of the illumination, radicals are formed but conversion is hindered because some ppm of oxygen solved in the material inhibit these radicals. After all oxygen is neutralized, the rest of the photoinitiator is transformed to radicals and parallel to this transformation conversion starts. This region in the conversion curve is characterized by constant radical formation and formation of C–C single bonds by polymerization which is correlated to a viscosity change of the material. Constant polymerization rate takes place up to the so-called gel point. Radicals loose their mobility because of the high viscosity of the medium and the reaction rate is controlled by the diffusion rate of rest radicals and polymerizable organic groupings. This so called gel point can be compared to the glass transition region for pure organic thermoplastic materials. If the inorganic polymer chains can be regarded as inorganic oligomer and polymer chains, which was indicated by NMR measurements, the gel point, and thereby the freezing in of the mobility of organic and inorganic monomer and polymer species should be overcome by heat treatment of the material during UV-polymerization. Results for C=C conversion in case of such a heat treatment are shown in Figure 6. As can be seen, conversion up to 90% can be obtained by temperature treatment at 100°C in comparison to 20% at room temperature if conversion of C=C double bonds is measured after a constant time of 10 min.

Every double bond conversion and as a consequence every polymerization of methacrylate based composites is directly connected to a polymerization shrinkage. The reason for polymerization shrinkage is the fact, that the distance between the monomer molecules and the resulting dimer in case of the used system MPTS/ZR/MAS is reduced during polymerization. The intermolecular distance between the base components is in the range of 3-4 Å (van der Waals forces) and reduces to 1.54 Å which corresponds to the distance of the C–C single bond. Parallel, the bonding distance in the monomer component of the methacrylate is increased by 0.19 Å when the double bond converts to a single bond. These changes in bond length result in a volume contraction of the composite during photopolymerization. This polymerization shrinkage can be followed on line by using a Mach-Zehnder interferometer. An Ar^+-laser of 351 nm wavelength is used to initiate photopolymerization in a 10 μm thin gel film, a He–Ne laser of 633 nm wavelength, which does not contribute to photopolymerization is used as a probe laser. By this probe laser, in connection with the Mach-Zehnder setup, an interference pattern is formed which shifts in case of thickness changes and volume contraction can be followed on line. The results of such an experiment are shown in Figure 7.

The thickness changes show a single exponential decay and result in a constant thickness after a characteristic time which is dependent from laser intensity. A laser intensity of at least 0.64 W/cm^2 has to be used for the given initiator concentration (1 weight%) if the final shrinkage should be independent of laser intensity. But as a consequence, also the degree of polymerization has to be lower for lower laser intensities because a smaller amount of C=C double bond conversions contribute to

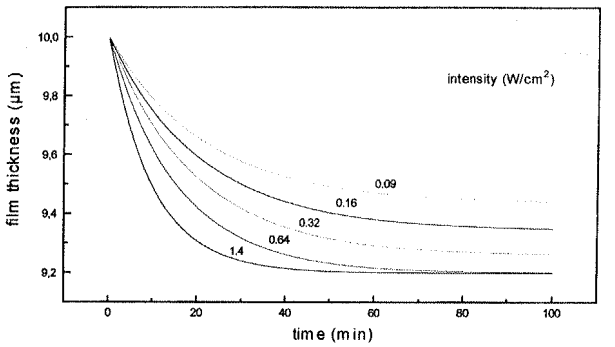

Figure 7. – Thickness changes of a thin gel film of the system MPTS/ZR/MAS during photopolymerization for different laser intensities.

the final shrinkage. The determination of time dependent C=C conversion as a function of laser intensity is a fundamental result for further processing like patterning and development by solvents to get three-dimensional structures.

Calculating double bond conversion IR-spectroscopically in our setup does not allow to follow the conversion process in real time. Therefore the well known technique of "Forced Rayleigh Scattering" (FRS), which was developed for dye doped polymer systems where the dyes act as tracer molecules and allow the measurement of diffusion rates of the polymer species was used. The experimental setup is shown in Figure 8.

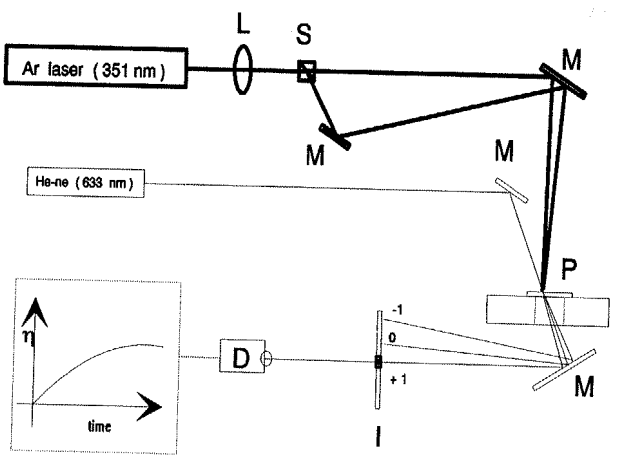

Figure 8. – Scheme of FRS experimental setup.

The FRS experiment consists of a laser beam of 351 nm in wavelength which is divided into two beams of exactly the same power by a beamsplitter S. By a directional mirror M these two beams interfer and form an interference pattern of periodic change of illumination on the sample. This special modulation of intensity in the interference region is adjusted by the angle between the two polymerizing beams. For the given setup, an angle of 6,7 degrees was choosen which corresponds to a periodicity of 3 μm of the spatial intensity modulation. As was seen in the on-line shrinkage experiment, laser intensity up to a threshold leads to differences in the degree of polymerization. If local polymerization with periodic modulation of degree of polymerization occurs in the sample, both the index of refraction (n) and the thickness (d) will change with the same periodicity. These changes in optical thickness (nd) result in a phase shift and a phase grating is built up which acts as a diffraction grating and the diffraction pattern can be visualized by a second laser beam of a wavelength which is not absorbed by the material. For the given experimental setup, a He-Ne laser of 633 nm wavelength was choosen. The intensity of the first diffraction order for this probe beam can be measured time dependent by a photodiode (D). A typical result is shown in Figure 9.

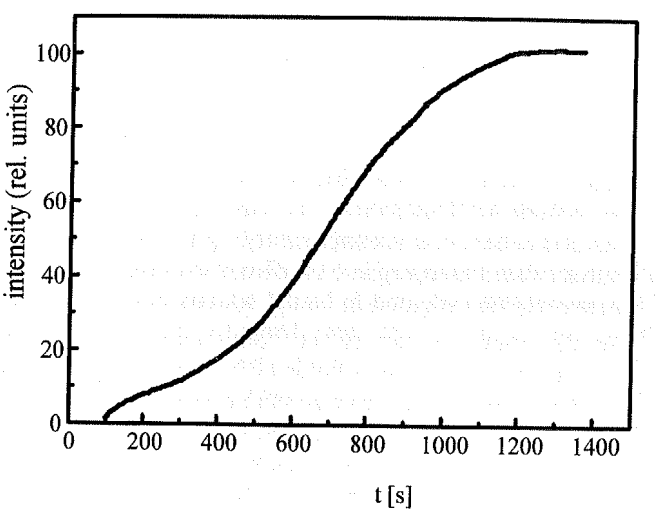

Figure 9. – Typical diffraction efficiency read in real time measured by FRS.

The shape of the curve is very similar to the one which was measured IR-spectroscopically in case of the conversion behavior. Also three regions can be distinguished: period of inhibition, period of radical formation and double bond conversion and a period of saturation after a gel point. The time dependent changes of the diffracted intensity $I(t)$ in the radical formation and conversion region can be approximated by an exponential function of the form (equation 3).

$$I(t) = \left(A + B \exp -\frac{t}{\tau}\right)^2 + C \qquad (3)$$

A and C are coherent and incoherent scattering backgrounds, B is a contrast factor and τ is a

characteristic relaxation time of the process which is responsible for signal changes. In case of FRS, the measured relaxation time corresponds directly to a diffusion coefficient D and the relation between τ and D is given by equation 4.

$$\tau^{-1} = 4\pi^2 D/\Lambda^2 \quad (4)$$

If the relaxation time of the investigated process and the grating period Λ of the diffraction grating are known, the diffusion coefficient can be calculated. If the relaxing species has pure diffusive character, the diffusion coefficient will show an Arrhenius behavior of the form (equation 5).

$$\ln D = \ln D_0 - E_A/kT \quad (5)$$

and the activation energy can be calculated. The experimental results of temperature dependent diffusion coefficients are shown in Figure 10. An activation energy of 29 kJ/mol is determined, which is typical for side chain relaxations of organic polymer systems.

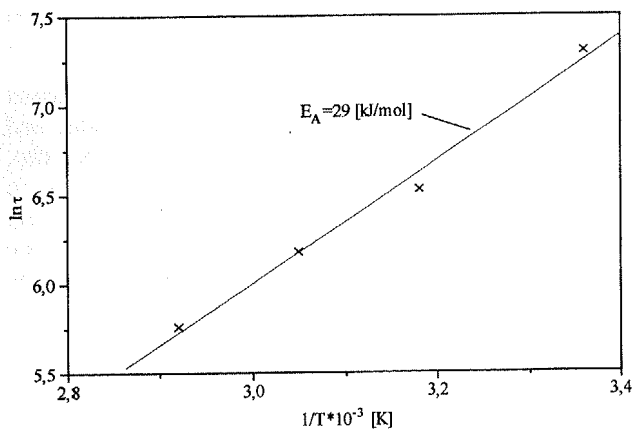

Figure 10. – Arrhenius plot of temperature dependent relaxation times.

Starting from this basic understanding of the system MPTS/ZR/MAS, thin films were prepared by dip and spin coating to measure surface roughness, optical losses and to investigate patternability to fabricate micro-structures. Surface roughness was determined by interferometric methods to be less than 1.5 nm rms which is a promising value for waveguide applications. Optical losses were determined by prism coupling combined with digital image processing which does not allow to measure optical losses less then 0.5 dB/cm. The system MPTS/ZR/MAS shows optical losses, which cannot be resolved by this technique which means than optical losses have to be less than the resolution of this technique of 0.5 dB/cm. To be able to produce buffer, waveguiding film and gladding material just by changing the index of refraction of the material, different composites were prepared by changing the ZR/MAS content of the composite (Fig. 11).

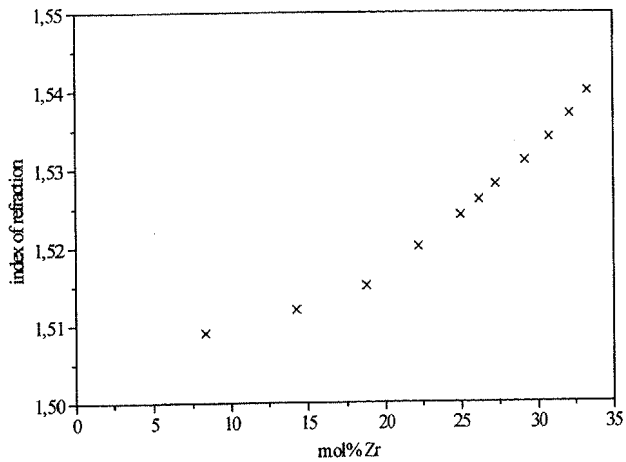

Figure 11. – Index of refraction in dependence of mol % ZR/MAS in MPTS.

Examples for practicle applications

The polymerization behavior in combination with deformability of the material in the gel state can be used for a variety of different patterning techniques. Beside simple structures like diffraction gratings or strip waveguides also complex shapes like Fresnel lenses can be prepared by adjusting the patterning techniques to the material characteristics.

Maskaligner techniques

Maskaligner techniques are used to produce complex structures by a single illumination step. A mask which is fabricated f.e. by X-ray lithography allows to polymerize regions of the material, where the mask is not covered with chromium. The film can be in hard contact or in near contact to the mask, which depends on the durability of the film because adhesion between the mask and the film has to be avoided. But the resolution of the obtained structure is strongly influenced by this distance, as diffraction effects will smear the exact profile in case of only near contact. Therefore, resolutions smaller than 1 μm can only be obtained in case of hard contact. The film has to be prepolymerized to a degree which prevents adhesion. An other advantage lies in the circumstance, that also round profiles can be produced by optimizing the polymerization and subsequent development step to get a three-dimensional pattern. A result of such an optimized processing is shown in Figure 12, where an array of

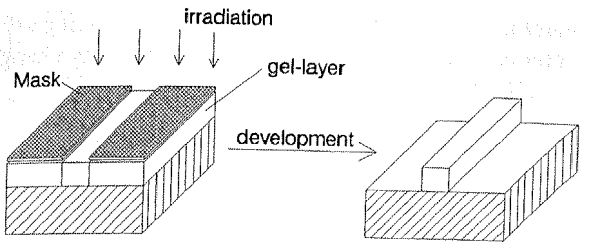

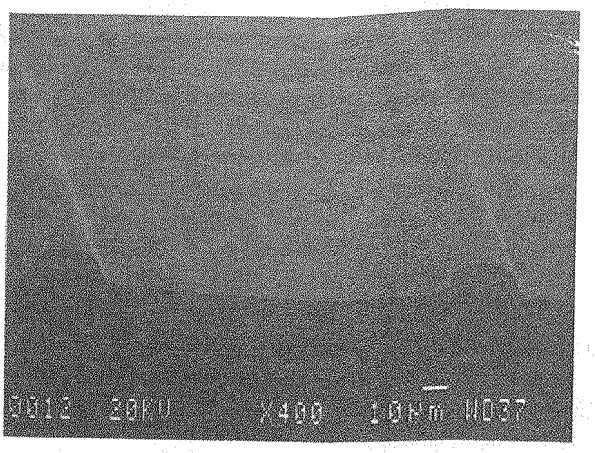

Figure 12. – Scheme of maskaligner experiment and obtained result after optimized polymerization and development step.

two strip waveguides was produced with rounded edges which is preferable for the connection with optical glas fibres to minimize coupling losses. The used material is a MPTS/ZR/MAS composite of the composition (10/1/1) in mol %. The patterned waveguides have typical dimensions of multi mode applications, which can be used in communication technology.

Direct laser writing of strip waveguides

In the direct laser writing experiment (Fig. 13), a laser beam (1) passes a beam expander (2) and is directed by a mirror (3) to a lens (4) which focuses the beam on the gel film (9) on a substrate which can be moved freely by a $x - y$ stage (10) on an optical table (12). A closed chamber (11) allows to use different atmospheres to eliminate inhibition by oxygen. The writing process can be followed by an endoscope (7) and a laser beam profilometer (6) to be able to correlate the used beam profile and the laser written pattern. After a development step, in which the unpolymerized material is dissolved by an alcohol, a three-dimensional structure is obtained. As can be seen in Figure 13, also rectangular structures are patternable, if laser intensity and moving velocity of the sample are correctly adjusted. In contrast to the maskaligner technique, the direct laser writing experiment has the advantage that the setup is very flexible to produce different patterns on the substrate and is therefore the better choice for material development and process optimization.

Another example for the combination of the direct laser writing experiment with formation of buffer and gladding layers is given in Figure 14. In a first step, the substrate was coated with a buffer layer to be independent of the index of refraction of the substrate material and to minimize surface scattering by substrate roughness. This film was polymerized as a whole by a Beltron UV curing apparatus with 2400 W power. In a second step, a film of a material with higher index of refraction was coated, laser patterned and the not polymerized regions were dissolved by an alcohol. The gladding material, again with lower index

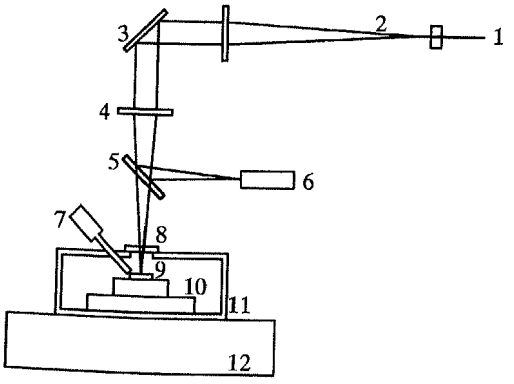

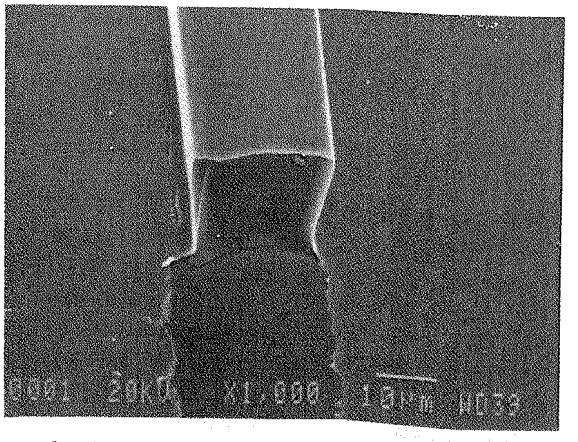

Figure 13. – Scheme of the direct laser writing experiment and a written structure after development with rectangular shape.

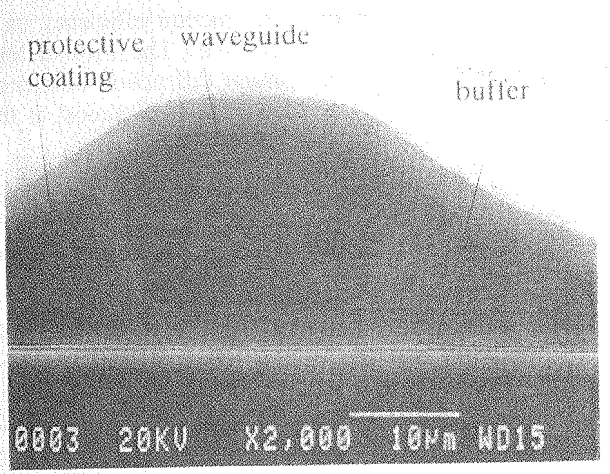

Figure 14. – SEM-micrograph of a sandwich buffer/strip waveguide/protective coating of the composites (10/3/3), (19/8/8), (19/3/3).

of refraction, was coated and hardened as it was the case for the buffer material. As the used material shows high scratch resistance and stability against alcohol or water after polymerization, these gladding coatings are good candidates to protect the waveguiding material from environmental and mechanical damage.

Embossing of micro lenses and diffraction gratings

Embossing is a very attractive technique to produce structures in industrial quantities. Once a stamper is prepared, it can be used to make replicas just by pressing this stamper in the material. But this material has to fullfill several requirements which limit this processing technique to very few material classes. For the given MPTS/ZR/MAS system, mechanical properties in the gel state can be varied in a wide range by adding a solvent or by small prepolymerization to adjust the viscosity and mechanical properties to the embossing process. The material has to be deformable to follow the shape of the stamper, but it has to be viscous enough not to spread completely. A silica substrate is coated with a thin film, solvent is evaporated and the film is defined prepolymerized. The stamper, which is in our experiment a glass stamper with 2400 lines/mm grating, is pressed on the film and polymerization is completed during the embossing step. After the stamper is removed, the negative of the stamper remaines in the film as patterned structure. Figure 15 shows a result of an embossed grating of 2400 lines/mm in the described MPTS/ZR/MAS system. Such gratings are used in integrated optics as couple gratings or fanout elements.

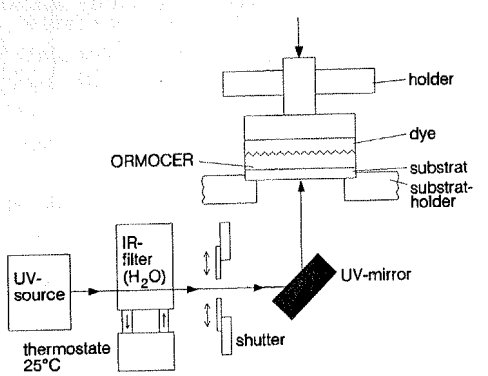

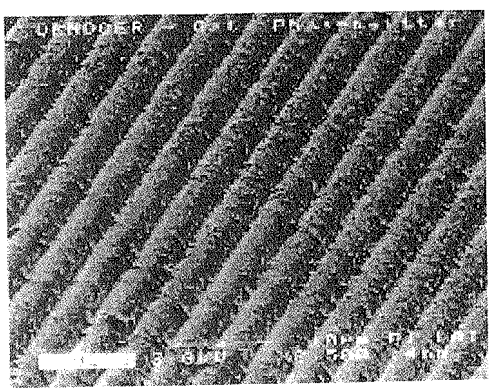

Figure 15. – Scheme of the embossing process and obtained grating with 2400 lines/mm.

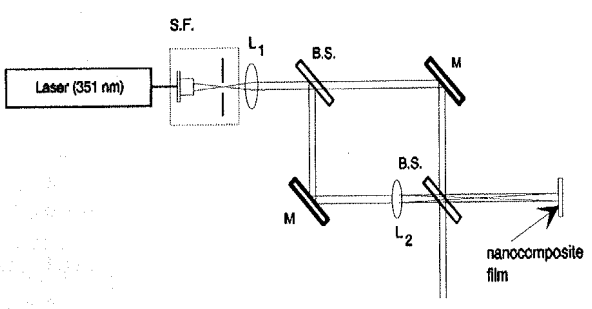

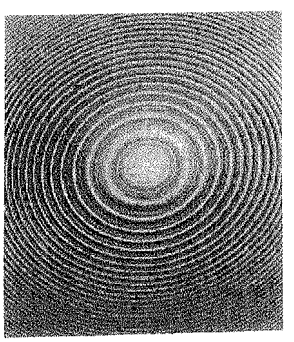

Figure 16. – Experimental setup for the fabrication of Fresnel-lenses (L: lens, M: mirror, BS: beam-splitter, SF: spatial filter).

Other structures like micro lenses with defined focal length and diameter can be obtained by this embossing technique. In the future it is planed to produce micro lens arrays by this technique by changing process parameters (local thermal polymerization) and emboss processing.

Holographic interference techniques for the production of Fresnel micro lenses

By definition a Fresnel zone plate, or so-called Fresnel lens, is an optical device with a surface modulation equal to rλf, where λ is the wavelength of the illuminated light and f is the principal focal length of the zone plate. A Mach-Zehnder interferometer is used to modulate the beam of a coherent light source (Ar^+-laser, λ=351 nm). The interference pattern is built up by an object wave with spheric wavefront (produced by L_2) and a planar wavefront. These two beams interfere at the location of the sample and concentric rings of maximum interference intensity lead to a degree of polymerization of almost sinusoidal form. Different interference pattern and thereby different Fresnel lenses can be produced by changing the sample position or the focal length of the lens system L_2. The principal experimental optical setup to fabricate Fresnel zone plates by laser interference technique is shown in Figure 16.

The theoretical maximum of diffraction efficiency of a thin phase zone plate is about 34%. The Fresnel lens presented here shows a maximum diffraction efficiency of 29% for the first order focus which is almost at the theoretical one.

Micro Fresnel lenses play an important role in the field of optical information, communication storage systems like optical disks, facsimile transmission or collimation units for laser diodes.

These examples show, that patternable organic- inorganic nanocomposites with low optical losses can be produced by reaction control and optimized synthesis procedure. Surface treatment of nanoparticles in combination with chemically controlled condensation is a powerful tool to prepare organic-inorganic hybrid materials with high potential for applications in integrated optics.

Acknowledgments

The authos wish to thank Dr. V. Gerhard and Dr. R. Kasemann for the IR-spectroscopic and NMR investigations. Thanks to Mr. F. Tiefensee and Mr. P.W. Oliveira for laser patterning and Dr. N. Merl for embossing investigations. The financial support of the government of the Saarland is gratefully acknowledged.

References

[1] Sanchez C., *Proc. 3rd Eurogel Conference*, December 1-4, 1992, Colmar (in print).

[2] Leoy D., Einhorn S., Avrir Dr., *J. Non-Cryst. Solids*, 1989, **113**, 137.

[3] Hou L., *Proc. 1st Conference on Sol-Gel Productions*, October 10-13, 1993, Saarbrücken Trans. Tech. Publications, Aldermannsdorf/Switzerland (in print).

[4] Altmann J. C., Stone R. E., presented at *Am. Cer. Soc. Sym. proc. optical Materials Symposium*, Oct. 21-23, 1991, Washington.

[5] Reisfeld R., in *Sol-Gel Science and Technology*, Eds., Aagerter M. A., Gaffelicci M. Jr., Souza D. F., Zanotto E., World Science Publishing, Singapore 1989, p. 323

[6] Li C., Chung Y. J., Mackenzie J. D., Knobble E. T., presented at *Am. Cer. Soc. Symp. proc. Optical Materials Symposium*, Oct. 21-23, 1991, Washington.

[7] Klein L. C., Abramoff B., *Polym. Prep.*, 1991, **32**, 519.

[8] Prasad P. D., in *SPIE*, **1328**, *Sol-Gel Optics*, Eds., Mackenzie J. D., Ulrich D. R., SPIE, Bellingham, Washington, 1990, p. 168.

[9] Toghe M., Asuka M., Minami T., in *SPIE*, **1328**, *Sol-Gel Optics*, Eds., Mackenzie J. D., Ulrich D. R., SPIE, Bellingham, Washington, 1990, 125.

[10] Rodrigues D. E., Brennan A. B., Betrabet C., Wang B., Wilkes G. L., *Polym. Prep.*, 1991, **32**, 525.

[11] Spanhel L., Arpac E., Schmidt H., *J. Non-Cryst. Solids*, 1992, 148, 657.

[12] Sanchez C., *J. Non-Cryst. Solids*, 1992, **147**, 1.

[13] Rinn G., Schmidt H., in *Proc. of the 2nd International Conference Ceramic Powder Processing Science*, Eds., Hauser H., Messing G. L., Hirano S., Deutsche Keramische Gesellschaft, Köln, 1989.

[14] Strehlow P., *J. Non-Cryst. Solids*, 1988, **107**, 55.

[15] Schmidt H., Krug H., Kasemann R., Merl N., Gerhard V., Tiefensee F., Brück S., in *Homage to Galileo*, Eds., Mazzoldi P., University of Padova, Italy, 1992, 303.

[16] Roncone R. L., Burke J. J., Weisenbach L., Zeliski B., *SPIE*, 1590, 1991.

[17] Schmidt H., Krug H., Kasemann R., Tiefensee F., *SPIE*, 1590, 1991, p. 36.

[18] Krug H., Tiefensee F., Oliveira P. W., Schmidt H., *SPIE*, 1758, 1992, p. 448.